Numerical investigation of spin-torque using the Heisenberg model

C. Schieback[1], M. Kläui[1], U. Nowak[2], U. Rüdiger[1], and P. Nielaba[1,a]

[1] Fachbereich Physik, Universität Konstanz, 78457 Konstanz, Germany
[2] Department of Physics, University of York, York YO10 5DD, UK

Received 8 October 2006 / Received in final form 22 December 2006
Published online 2 March 2007

Abstract. We present numerical calculations of the spin transfer torque resulting in current-induced domain wall motion. Rather than the conventional micromagnetic finite difference or finite element method, we use an atomistic/classical Heisenberg spin model approach, which is well suited to study geometrically confined domain walls. We compute the behaviour of domain walls in a one dimensional chain when currents are injected using adiabatic and non-adiabatic spin torque terms. Our results are compared to analytical calculations and are found to agree very well for small current densities. At larger current densities deviations are observed, which can be attributed to the approximations used in the analytical calculations.

PACS. 72.25.Ba Spin polarized transport in metals – 72.25.Pn Current-driven spin pumping

1 Introduction

Domain walls and magnetisation reversal by domain wall motion have recently become the focus of interest by allowing us to address fundamental physical questions, such as the geometry dependent spin structure [1,2], pinning of domain walls at constrictions [3–8] and the details of the domain wall propagation processes [9,10]. Additionally, devices based on domain walls have been suggested for data storage and logic [11,12]. Rather than using conventional magnetic fields to move domain walls, recently current-induced domain wall motion [13–24] has received much attention, since it opens up a route for simple device fabrication, as no field-generating strip lines are necessary. Devices based on current-induced domain wall motion have also been put forward, the most prominent being the racetrack memory [22]. Apart from possible applications, the interplay between spin currents and domain walls in magnetic nanostructures is of fundamental interest, since the basic physical mechanisms involved are not completely understood. Experimentally spin torque effects on domain walls were observed early on (see e.g. [15]), and recently controlled current-induced motion of single domain walls in magnetic nanostructures has been achieved. Several important aspects like domain wall velocities [16,17], critical current densities [18–20,24], thermally assisted motion [21], and the impact of currents on the domain wall spin structure [17] have been addressed.

[a] e-mail: peter.nielaba@uni-konstanz.de

One approach to studying and understanding domain wall spin structures and current-induced domain wall motion is using computational methods. Using various numerical methods, this has been very successful in recent years in explaining experimental observations, such as domain structures, reversal modes and other magnetic effects [25–27]. The micromagnetic approach, where the time integration of the standard Landau-Lifshitz (and Gilbert) equation [28] is carried out on a square (or cubic) lattice has been become very popular with the advent of the freely available OOMMF software [29] and other commercial packages. While many experimental results could be reproduced using this software, some of the most exciting aspects of nanomagnetism could not be investigated, namely the influence of temperature and the spin transfer torque effect that leads to current-induced domain wall motion for geometrically confined domain walls.

Micromagnetic calculations including a white noise fluctuating field to account for the effects of temperature encounter the following problem: due to the cell size of usually just below the exchange length (a few nanometer in many 3d metals), the thermally excited spin wave spectrum is cut off at the wavelength that corresponds to the cell size. An atomistic simulation allows to reproduce thermal effects with higher accuracy and such thermal effects have been shown to be of paramount importance for domain walls [4] and in the context of the spin transfer torque effect [30].

What is more, geometrically confined domain walls can contain changes in the spin structure at very short length scales [3,4]. In the usual micromagnetic approach, the

exchange energy is approximated by $(\nabla(m))^2$, which is the first order Taylor expansion of the dot product and only valid for small angles between neighbouring cells [26,27]. In order to avoid this problem, an atomistic/classical spin model approach can be used, where the exchange energy is calculated as the dot product [4].

Finally, the standard Landau-Lifshitz-Gilbert equation does not account for the spin transfer torque effect, which leads to current-induced domain wall motion and so it has to be extended. Theoretically, the phenomenon of current-induced domain wall motion has been long known [13,14] but the underlying theory of interaction between current and magnetisation is still controversial. Different approaches have been suggested, in the ballistic limit [31,32] as well as in the diffusive limit [14,32]. The assumption that the spin of the charge carriers follows the local magnetisation leads to the introduction of an adiabatic torque into the Landau-Lifshitz-Gilbert equation of magnetisation dynamics [32–34]. Motivated by large discrepancies between experiment and theory, a non-adiabatic term was introduced [35,36]. He et al. [37] predicted that the (non)-adiabaticity parameter of the spin torque strongly influences the combinations of field and current necessary to move a wall and so a study of domain wall motion as a function of current and field might help to ascertain this parameter if simulations and experimental results are available for the same geometry. Furthermore, a discrepancy between room temperature measurements and 0 K calculations of the domain wall velocity exists [16,17,35,36]. To reveal possible explanations, temperature dependent measurements and calculations of the critical current density and the velocity is a key issue to determine the temperature dependence of the spin torque effect efficiency.

Thus a possible route to simulations of current-induced domain wall motion of highly confined walls at variable temperature, which we present in this paper is an atomistic simulation using an atomistic/classical spin model approach [25] and including the adiabatic and the non-adiabatic spin torque terms. We study first the simplest case of a one dimensional chain at 0 K, which can be calculated analytically and compare the results of our approach with the analytical predictions and discuss possible deviations.

2 Model, simulation

We consider a classical Heisenberg model: the magnetic moments are located on a cubic lattice with nearest neighbours ferromagnetic exchange coupling.

$$\begin{aligned}\mathcal{H} = &- J\sum_{\langle ij\rangle} \boldsymbol{S}_i \cdot \boldsymbol{S}_j - d_x \sum_i S_{x,i}^2 - d_y \sum_i S_{y,i}^2 \\ &- \frac{w}{2}\sum_i \sum_{i\neq j} \frac{3(\boldsymbol{S}_i \cdot \boldsymbol{e}_{i,j})(\boldsymbol{e}_{i,j} \cdot \boldsymbol{S}_j) - \boldsymbol{S}_i \cdot \boldsymbol{S}_j}{r_{i,j}^3} \\ &- \mu_s \boldsymbol{B} \cdot \sum_i \boldsymbol{S}_i \end{aligned} \quad (1)$$

$\boldsymbol{S}_i = \boldsymbol{\mu_i}/\mu_s$ denotes the three-dimensional magnetic moment of unit length with $\mu_s = |\boldsymbol{\mu_i}|$, J with $J > 0$ the ferromagnetic exchange coupling constant, d_x and d_y the anisotropy constants. For $d_x > d_y > 0$ the x-axis is a magnetically "easy" axis and the y-axis is a magnetically "middle" axis, $w = \mu_0\mu_s^2/(4\pi a^3)$ is the strength of the dipole-dipole interaction, $r_{i,j}$ the distance between the magnetic moments, i and j are in units of the lattice constant a, $\boldsymbol{e}_{i,j}$ the unit vector in the direction of $\boldsymbol{r}_{i,j}$ and $\boldsymbol{B}$ the external magnetic field.

The first term of the Hamiltonian describes the isotropic exchange interaction between neighbouring magnetic moments. With a ferromagnetic exchange interaction the magnetic moments align parallel. The second and third term describe two anisotropy terms. The magnetic moments thus preferentially orient themselves in the xy-plane. The forth term of the Hamiltonian describes the long-ranged dipole-dipole interaction leading to shape anisotropy. These interactions compete and determine the order of the magnetic moments in a system. The last term of the Hamiltonian describes the coupling of magnetic moments to an external magnetic field $\boldsymbol{B}$ (Zeeman term).

The dynamics of the system, respectively the equation of motion of the magnetic moments $\boldsymbol{S}_i$ is governed by the Landau-Lifshitz-Gilbert (LLG) equation [28]:

$$\frac{\partial \boldsymbol{S}_i}{\partial t} = -\frac{\gamma}{(1+\alpha^2)\mu_s} \boldsymbol{S}_i \times \left[\boldsymbol{H}_i(t) + \alpha(\boldsymbol{S}_i \times \boldsymbol{H}_i(t))\right] \quad (2)$$

$\boldsymbol{H}_i = -\frac{\partial \mathcal{H}}{\partial \boldsymbol{S}_i}$ are the effective fields, α is the dimensionless Gilbert damping constant, and $\gamma = g\mu_B/\hbar$ is the gyromagnetic ratio. The first term of the LLG equation describes the precession of the magnetic moment $\boldsymbol{S}_i$ within the effective field $\boldsymbol{H}_i$. The second term describes the relaxation of the magnetic moment.

To take thermal fluctuations into account, a time dependent thermal noise term $\boldsymbol{\zeta}_i(t)$ can be added into the effective field term $\boldsymbol{H}_i$ [38].

$$\boldsymbol{H}_i(t) = -\frac{\partial \mathcal{H}}{\partial \boldsymbol{S}_i} + \boldsymbol{\zeta}_i(t) \quad (3)$$

$\boldsymbol{\zeta}_i(t)$ possesses the properties of white noise:

$$\langle \boldsymbol{\zeta}(t)_i \rangle = 0 \quad (4)$$

$$\langle \zeta_i^\nu(t)\zeta_j^\Theta(t')\rangle = 2\frac{\alpha\mu_s}{\gamma} k_B T \delta_{i,j}\delta_{\nu,\Theta}\delta(t-t') \quad (5)$$

Θ, ν are the Cartesian coordinates, k_B is the Boltzmann constant, and T is the temperature. In the simulation, thermal fluctuations are represented by Gaussian distributed random numbers.

The numerical time integration of the LLG equation has been carried out by using a Heun-method [39,40].

To take a spin-polarised current in the x-direction into account we follow the approach presented in [34–36,41]. In these studies the interaction between electron spins and magnetic moments have been treated by additional terms

in the implicit LLG equation.

$$\frac{\partial \boldsymbol{S}_i}{\partial t} = -\frac{\gamma}{\mu_s}\boldsymbol{S}_i \times \boldsymbol{H}_i(t) + \alpha \boldsymbol{S}_i \times \frac{\partial \boldsymbol{S}_i}{\partial t} - u_x \frac{\partial \boldsymbol{S}_i}{\partial x} + \beta u_x \boldsymbol{S}_i \times \frac{\partial \boldsymbol{S}_i}{\partial x} \quad (6)$$

u_x is given by $u_x = j_e P g \mu_B/(2eM_s)$ with j_e the current density, P the polarisation, M_s the saturation magnetisation and β a constant non-adiabaticity parameter. u_x is in units of a velocity and proportional to the applied current. The equation can be easily transformed to the explicit LLG equation, which is used in our simulations.

$$\frac{\partial \boldsymbol{S}_i}{\partial t} = -\frac{\gamma}{(1+\alpha^2)\mu_s}\boldsymbol{S}_i \times \left[\boldsymbol{H}_i(t) + \alpha(\boldsymbol{S}_i \times \boldsymbol{H}_i(t))\right] + \frac{1+\beta\alpha}{(1+\alpha^2)} u_x \boldsymbol{S}_i \times \left[\boldsymbol{S}_i \times \frac{\partial \boldsymbol{S}_i}{\partial x}\right] - \frac{\alpha-\beta}{(1+\alpha^2)} u_x \boldsymbol{S}_i \times \frac{\partial \boldsymbol{S}_i}{\partial x}. \quad (7)$$

The extended LLG equation consists now of four terms. The last two terms include the effect of a spin-polarised current on the dynamics of the magnetic moments.

3 Numerical results

In the following we present results from a system with a spin chain ($d = 1$) along the x-direction, which is the simplest model, which also allows comparison to analytical calculations. The system size was chosen to be 513 or 1025 lattice sites. The simulations were all first performed at 0 K with ferromagnetic exchange coupling and anisotropy constants $d_x/J = 0.01$ and $d_y/J = 0.005$, Gilbert damping constant $\alpha = 0.02$, and $w = 0$. The external magnetic field was set to zero. For comparison of wire geometries [41,34] with analytical 1D predictions, the effects of the exchange interaction and the shape anisotropy due to the dipolar interaction were included in a so-called effective anisotropy term in the 1D model. This effective anisotropy term has the same form as our anisotropy terms have.

In the simulations a planar domain wall separating two head to head domains along the chain direction (x-direction) was considered.

$$\boldsymbol{S}(x) = -\tanh\left(\frac{x}{W}\right)\boldsymbol{e}_x + \frac{\cos(\phi)}{\cosh(\frac{x}{W})}\boldsymbol{e}_y + \frac{\sin(\phi)}{\cosh(\frac{x}{W})}\boldsymbol{e}_z \quad (8)$$

here W is the domain wall width and ϕ is the out-of-plane angle. The initial magnetisation configuration is a stable planar domain wall in the xy-plane ($\phi = 0$ and $W = W_0$). The magnetic moments at the ends of the wire were fixed along the x respectively along the $-x$ direction. To determine the position, the width and the out-of-plane angle of the planar domain wall the S_x and S_y components of the chain were fitted using equation 8.

The following simulation results of adiabatic and non-adiabatic spin torque effects are obtained by using a Heisenberg model, equation (1). We compare to related recent results from the literature, where micromagnetic finite difference approaches and analytical calculations had been chosen.

In reference [41] a current along the x-direction is applied to a wire with a standard in-plane transverse domain wall separating two head to head domains along the wire direction (x-direction). Analytical and numerical results [41] for the velocity, reversible displacement x_{dw}, the out-of-plane angle and the deformation of the domain wall have been obtained for the case of a low current u_x below the so called Walker breakdown [42] and $\beta = 0$. For domain walls driven by an external magnetic field the Walker breakdown is a well known phenomenon [10,42,43]. Above a critical external magnetic field along a wire precession of the domain wall around the external field occurs and the domain wall velocity decreases. A similar phenomenon occurs in current-driven domain wall motion [35,36]. For current densities below the Walker breakdown, the domain wall only moves a distance $x_{dw} \propto u_x$ and is tilted out of the xy-plane by an angle $\phi \propto u_x$ until it stops. Additionally the original domain wall was distorted according to $W/W_0 \approx 1 - C \cdot u_x^2$. In our simulations we observe for low current u_x and $\beta = 0$ that the domain wall moves along the wire to a maximum displacement and then stops. Simultaneously the magnetic moments of the wall tilt out of the easy plane until a maximum out-of-plane angle is reached. This behaviour can be explained by looking at the four terms of the extended LLG equation. The spin torque is balanced by an "internal" torque due to the anisotropy contribution to the effective field. The displacement in the x-direction given by the third term of the LLG equation is balanced by the precessional term which acts in the opposite direction. The forth term which tilts the magnetic moments out of the easy plane is balanced by the relaxation term. In Figures 1–3 we show results of our simulations for the displacement, the out-of-plane angle and the distortion of the domain wall as a function of u_x. Good agreement with the low current predictions is found, for larger currents we find deviations. The analytical calculations assume that the domain wall shape remains in the standard transverse domain wall which is only valid for small currents. So deviations from the analytical predictions for lager currents are expected.

In [34] an approximate analytical prediction for the long term domain wall velocity $\langle v \rangle$ as a function of u_x has been derived: $\langle v \rangle = \sqrt{u_x^2 - u_c^2}/(1+\alpha^2)$ for values of u_x exceeding a critical effective velocity u_c respectively exceeding a critical current. Simulations [34] of a wire with a transverse domain wall showed a periodic antivortex nucleation and annihilation for $u_x > u_c$. As described above we observe for low current u_x in long term simulations no continuous domain wall motion. For larger currents u_x the spin torque cannot be any longer balanced by the "internal" torque due to anisotropy effects. The domain wall motion occurs additionally to a precession of the magnetic moment around the x-direction. As shown in Figure 4 for the case $\beta = 0$ we also observe a critical value for u_c. The analytical predictions of $\langle v \rangle$ have been very

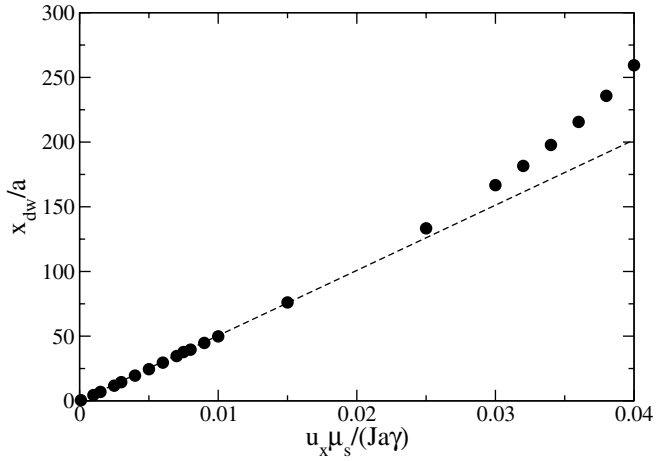

Fig. 1. Simulation results (symbols) for the final x-displacement x_{dw} of the domain wall as a function of u_x. The line shows a linear fit for small u_x. Parameters: $\alpha = 0.02, \beta = 0$.

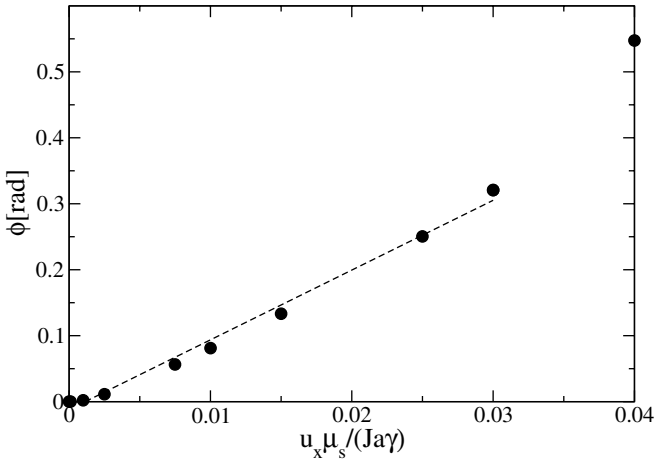

Fig. 2. Simulation results (symbols) for the final out-of-plane angle ϕ as a function of u_x. The line shows a linear fit for small u_x. Parameters: $\alpha = 0.02, \beta = 0$.

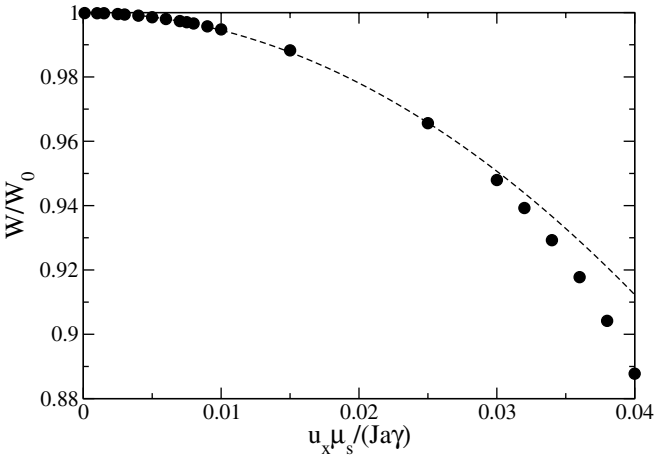

Fig. 3. Simulation results (symbols) of the reduction of the width of the domain wall as a function of u_x. The line shows the fitting function $W/W_0 = 1 - C \cdot u_x^2$ for small u_x. Parameters: $\alpha = 0.02, \beta = 0, C = 54.84$.

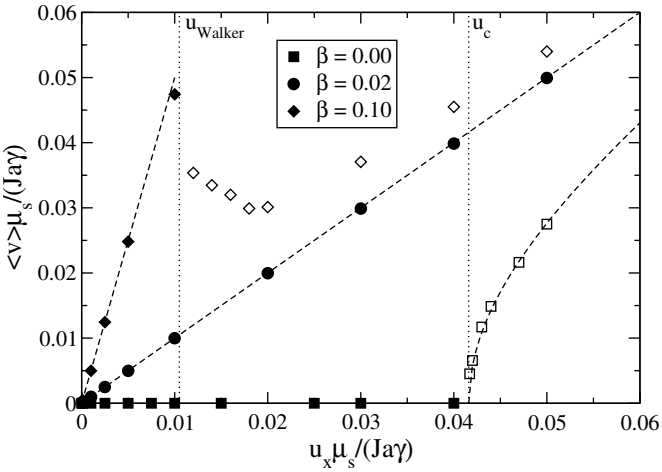

Fig. 4. Simulation results (symbols) for the long term domain wall velocity $\langle v \rangle$ as function of u_x for different values of β. The dashed lines show fits to analytical predictions [34,36]. Open symbols denote that the domain wall rotates around the x-axis. Parameters: $\alpha = 0.02$.

well reproduced by our simulations. As we are considering in our simulation a spin chain, the equivalent of the wall transformation discussed above is the rotation of the domain wall around the x-axis, which we indeed observe.

The effects of non-adiabatic spin torque contributions ($\beta \neq 0$) have been investigated as well. For comparison with analytical predictions of [36] we assumed the non-adiabaticity parameter β to be a constant value throughout the system. In [44] non-local contributions to β, which are strongly correlated to the domain wall width, are predicted. Including this will be reserved for future studies. In Figure 4 we present results for the long term domain wall velocity as a function of u_x for different values of β. For the case $\beta = \alpha$, the last term off the LLG equation vanishes. The magnetic moments are not tilted out of the easy plane. That means that no torque acts on the magnetic moments due to the precessional and relaxation part of the LLG equation. The magnetic moments are only influenced by the third term of the LLG which shift the domain wall along the wire and no transformations (rotation around the x-axis) occur. For the case of $\beta \neq \alpha$ for all values of u_x continuous domain wall motion is observed. Two regimes can be distinguished. For $u_x < u_{Walker}$ the velocity is given by $\langle v \rangle = \beta u_x / \alpha$ [36] as in the case of $\beta = \alpha$. For the case of $\beta = 0.1$ the maximum Walker velocity v_{Walker} is given by $v_{Walker} = 5 \cdot u_x$. The ratio between u_c and v_{Walker} is 0.0416/0.048 (0.867), which is in agreement to [36] where it is 600 m/s divided by 700 m/s (0.857) in the micromagnetic case and 1/1.25 (0.800) for the analytical calculation. Above u_{Walker} continuous rotation of the magnetic moments around the x-axis is found which initially leads to a lower domain wall velocity. Only at higher u_x the velocity starts to increase again. Good agreement with the results of [36,45] is obtained.

4 Conclusions

In conclusion we have shown that using an atomistic/classical spin model we can calculate the effects of the spin transfer torque. We compute the behaviour of domain walls in a one dimensional chain when currents are injected by the time integration of the Landau-Lifshitz and Gilbert equation including adiabatic and non-adiabatic spin torque terms. Very different behaviour is observed depending on the value of the non-adiabatic term. Our results are compared to analytical calculations and are found to agree very well for small current densities. At larger current densities deviations are observed, which can be attributed to the approximations used in the analytical calculations.

The general method outlined here contains temperature effects and the magnetic moments can be described on a more microscopic level using an atomistic lattice compared to standard micromagnetic finite difference approaches. Thus it is applicable to a broad range of interesting experimentally studied systems for geometries with extensions below the applicability of micromagnetic approaches. Our code is particularly well suited for highly confined domain walls with large magnetisation gradients and using an atomistic approach it allows to also include thermal effects. Thus we plan to apply it to the problem of current-induced motion of confined domain walls with the same geometries, which are studied experimentally. Due to the large computational cost, efforts are under way to perform these calculations using High Performance Computing facilities.

The authors thank R. Wieser for helpful discussions. The work has been supported by the Landesstiftung Baden-Württemberg and we thank the SSC, NIC and the HLRS for computer time.

References

1. R.D. McMichael, M.J. Donahue, IEEE Trans. Magn. **33**, 4167 (1997)
2. M. Laufenberg et al., Appl. Phys. Lett. **88**, 52507 (2006)
3. P. Bruno, Phys. Rev. Lett. **83**, 2425 (1999)
4. N. Kazantseva, R. Wieser, U. Nowak, Phys. Rev. Lett. **94**, 37206 (2005)
5. M. Kläui et al., Phys. Rev. Lett. **90**, 97202 (2003)
6. C.C. Faulkner et al., J. Appl. Phys. **95**, 6716 (2004)
7. M. Kläui et al., Appl. Phys. Lett. **87**, 102509 (2005)
8. A. Himeno et al., J. Appl. Phys. **99**, 08G304 (2006)
9. G.S.D. Beach et al., Nature Mater. **4**, 741 (2005)
10. Y. Nakatani et al., Nature Mater. **2**, 521 (2003)
11. R.P. Cowburn, Patents PCT/GB2003/001266, PCT/GB2004/000840 (2004)
12. D.A. Allwood et al., Science **309**, 1688 (2005)
13. L. Berger, J. Appl. Phys. **55**, 1954 (1984)
14. J.C. Slonczewski, J. Magn. Magn. Mater. **159**, L1 (1996)
15. P.P. Freitas, L. Berger, J. Appl. Phys. **57**, 1266 (1985)
16. A. Yamaguchi et al., Phys. Rev. Lett. **92**, 77205 (2004)
17. M. Kläui et al., Phys. Rev. Lett. **95**, 26601 (2005); M. Kläui et al., Appl. Phys. Lett. **88**, 232507 (2006)
18. J. Grollier et al., Appl. Phys. Lett. **83**, 509 (2003)
19. N. Vernier et al., Europhys. Lett. **65**, 526 (2004)
20. M. Kläui et al., Phys. Rev. Lett. **94**, 106601 (2005)
21. D. Ravelosona et al., Phys. Rev. Lett. **95**, 117203 (2005)
22. S.S.P. Parkin, U.S. patent 6,834,005 (2003)
23. A. Yamaguchi et al., Appl. Phys. Lett. **86**, 12511 (2005)
24. A. Himeno, S. Kasai, T. Ono, Appl. Phys. Lett. **87**, 243108 (2005)
25. U. Nowak, in *Annual Reviews of Computational Physics IX*, edited by D. Stauffer (World Scientific, Singapore, 2001), p. 105
26. H. Kronmüller, M. Fähnle, in: *Micromagnetism and the Microstructure of Ferromagnetic Solids*, Cambridge University Press (2003)
27. A. Aharoni, *Introduction to the theory of ferromagnetism,* (Clarendon Press, Oxford, 1996)
28. L.D. Landau, E.M. Lifshitz, Physik Z. Sowjetunion **8**, 153 (1935)
29. The OOMMF software is available at `http://math.nist.gov/oommf`
30. M. Laufenberg et al., Phys. Rev. Lett. **97**, 46602 (2006)
31. V.A. Gopar et al., Phys. Rev. B **69**, 14426 (2004)
32. G. Tatara, H. Kohno, Phys. Rev. Lett. **92**, 86601 (2004)
33. Z. Li, S. Zhang, Phys. Rev. Lett. **92**, 207203 (2004)
34. A. Thiaville, Y. Nakatani, J. Miltat, N. Vernier, J. Appl. Phys. **95**, 7049 (2004)
35. S. Zhang, Z. Li, Phys. Rev. Lett. **93**, 127204 (2004)
36. A. Thiaville, Y. Nakatani, J. Miltat, Y. Suzuki, Europhys. Lett. **69**, 990 (2005)
37. J. He, Z. Li, S. Zhang, J. Appl. Phys. **98**, 16108 (2005)
38. W.F. Brown, Phys. Rev. **130**, 1677 (1963)
39. J.L. Garcia-Palacios, F.J. Lázaro, Phys. Rev. B **58**, 14937 (1998)
40. C.W. Gardiner, *Handbook of Stochastic Methods* (Springer-Verlag, Berlin 1990)
41. Z. Li, S. Zhang, Phys. Rev. B **70**, 24417 (2004)
42. N.L. Schryer, L.R. Walker, J. Appl. Phys. **45**, 5406 (1974)
43. R. Wieser, U. Nowak, K.D. Usadel, Phys. Rev. B **69**, 064401 (2004)
44. J. Xiao, A. Zangwill, M.D. Stile, Phys. Rev. B **73**, 054428 (2006)
45. J. He, Z. Li, S. Zhang, Phys. Rev. B **73**, 184408 (2006)